JOURNAL OF MATERIALS SCIENCE 19 (1984) 1517–1521

Stress corrosion cracking of Al–Zn–Mg alloy AA-7039 by slow strain-rate method

YONG CHOI*, H. -C. KIM†, SU-IL PYUN*
*Department of Materials Science and Engineering and †Department of Physics, Korea Advanced Institute of Science and Technology, POB 150, Cheongryang, Seoul, Korea

The stress corrosion behaviour of Al–Zn–Mg alloy AA-7039 in an aqueous 3.5 wt % NaCl solution (pH = 1) was studied with the specimens under constant strain rate as function of ageing state and cold working. The tests were carried out at temperatures of 30 and 45° C and strain rates between 7.6×10^{-7} and 7.6×10^{-6} sec^{-1} and the apparent activation energy for mechanical deformation in oil and stress corrosion cracking (SCC) process in NaCl solution were determined. The fracture energy in NaCl solution under constant strain rate, as compared with experiments in oil, was lowered in the overaged specimens and markedly lowered in sequence of the peak-aged and the underaged specimens. The values of fracture energy for peak-aged and overaged specimens were nearly similar to those in oil at the higher strain rate of 7.6×10^{-6} sec^{-1}. The relative fracture energy was comparatively lowered in the fine-grained specimens, as compared to coarse-grained specimens. The apparent activation energy for mechanical processes in oil was found to be 103 kJ mol^{-1} in the peak-aged and 96.5 kJ mol^{-1} in the overaged specimens. Those for SCC processes in NaCl solution were 47.5 kJ mol^{-1} in the peak-aged and 51.5 kJ mol^{-1} in the overaged specimens. The results suggest that stress corrosion (SC) cracks are initiated by electrochemical dissolution of grain boundaries (gbs) and propagated by mechanical processes such as creep.

1. Introduction

Over the last few decades stress corrosion cracking (SCC) mechanism in Al–Zn–Mg and Al–Cu–Mg alloys has been studied mostly on the basis of SCC susceptibility–metallurgical variables such as precipitate (ppt) size and interparticle spacing in the grain boundaries (gbs) [1–4], distribution of matrix solute atoms (magnesium, zinc) in the gbs [5–9], precipitate free zone (pfz) width [10–13] and coherency of ppts in the grain [14–21]. However, it is extremely difficult to produce a given variation in one feature without a concomitant change in the other variables.

Several authors [22, 23] proposed the SCC mechanism based on the analysis of the activation energy by measuring stress corrosion (SC) crack propagation rate/or SCC failure time as a function of testing temperature. In contrast to constant load or constant strain methods, Parkins has introduced a constant strain-rate method [24, 25] and verified the existence of a minimum in relative fracture elongation/or relative fracture energy at the critical strain-rate range [26, 27].

The present study is aimed to separate mechanical from chemical contributions to the SC crack growth processes by comparing SCC resistance determined by the slow strain-rate method with those determined by the constant load method as a function of ageing stage and cold working.

2. Experimental procedure

The starting material was a commercially available plate of 10 mm thickness Al–Zn–Mg alloy AA-7039 of the following chemical composition (in wt %): 4.27% zinc, 2.76% magnesium, 0.257% manganese, 0.243% chromium, 0.157% iron, 0.072% titanium, 0.06% copper, 0.034% silicon, aluminium balance. The plate was hot-rolled at

0022–2461/84 $03.00 + .12

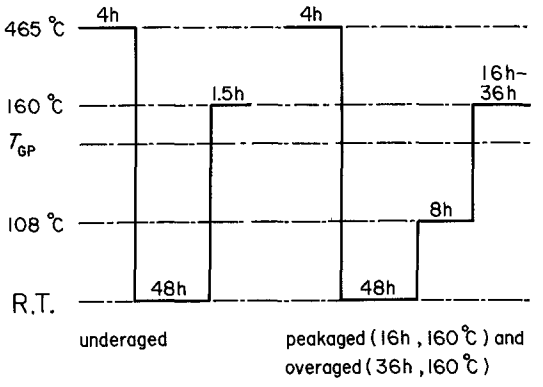

Figure 1 Heat treatments of specimens.

430° C, and the 33 and 75% cold-rolled to a thickness of 1 mm. SCC test specimens, similar to ASTM subsize tensile specimens of 1 mm thickness and 55 mm gauge length, were prepared from two different degrees of cold-rolled plates. The 33% cold-rolled specimens were solution treated at 465° C for 4 h in the $KNO_3/NaNO_3 = 1/1$ salt bath, resutling in a grain size of 44 μm, and the 75% cold-rolled specimens solution treated at 465° C for 50 min, resulted in a grain size of 22 μm, then quenched in water at 0° C. Both types of specimens were subjected to ageing treatments: 1.5 h at 160° C for underageing, two stages of treatments for peak-aged and overaged specimen, 8 h at 108° C followed by 16 and 36 h at 160° C, respectively (see Fig. 1).

Before the SCC tests, standard metallographic surface treatments were carried out and the specimens were then immersed in concentrated nitric acid for 30 sec, to reconstitute the oxide film. The SCC tests were carried out on an Instron testing machine with a 10 kN load cell at 30 or 45° C in a 3.5 wt% NaCl solution with its pH adjusted to 1.0 by means of hydrochloric acid.

3. Results and discussion

The variation of microhardness of 33% cold-rolled specimens with ageing time is presented in Fig. 2. The specimens aged in one stage at 160° C showed near constancy of microhardness with ageing time, while those aged in two stages showed significant age hardening.

Relative fracture energies [25, 26] of 33% cold-rolled specimens in NaCl solution and oil at 30 and 45° C, are illustrated in Figs. 3 and 4, respectively. All specimens showed a higher strain-rate dependence of relative fracture energy in the low strain rate ranges ($7.6 \times 10^{-7} \sim 1.6 \times 10^{-6}$ sec^{-1}, first

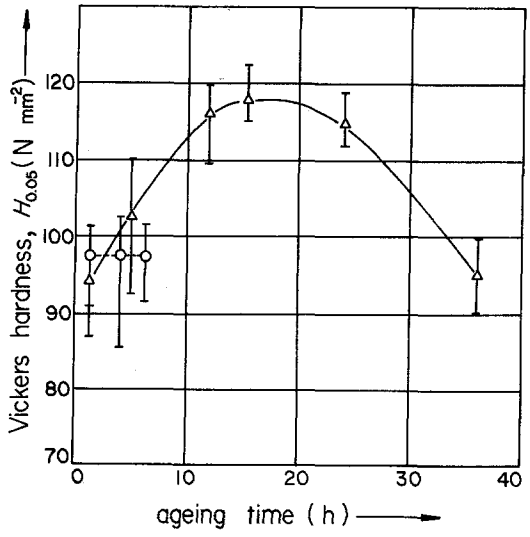

Figure 2 Variation of Vickers microhardness of 33% cold-rolled specimens with ageing time: ○ aged in one stage at 160° C; △ aged in two stages, 8 h at 108° C followed by various ageing times at 160° C.

stage) and a near invariant in the high strain rate ranges ($1.6 \times 10^{-6} \sim 7.6 \times 10^{-6}$ sec^{-1}, second stage).

The SEM fractography of the specimen tested at $\dot{\varepsilon} = 1.6 \times 10^{-6}$ sec^{-1} showed a transition of fracture mode from intercrystalline brittle fracture at the surface/subsurface to dimpled rupture in

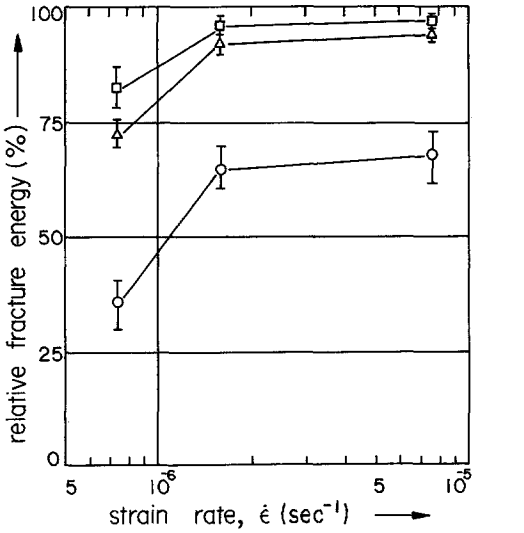

Figure 3 Strain-rate dependence of relative fracture energy in 3.5 wt% NaCl solution at 30° C, 33% cold-rolled specimens: ○ underaged in one stage 1.5 h at 160° C; △ peak-aged in two stages, 8 h at 108° C followed by 16 h at 160° C; □ overaged in two stages, 8 h at 108° C followed by 36 h at 160° C.

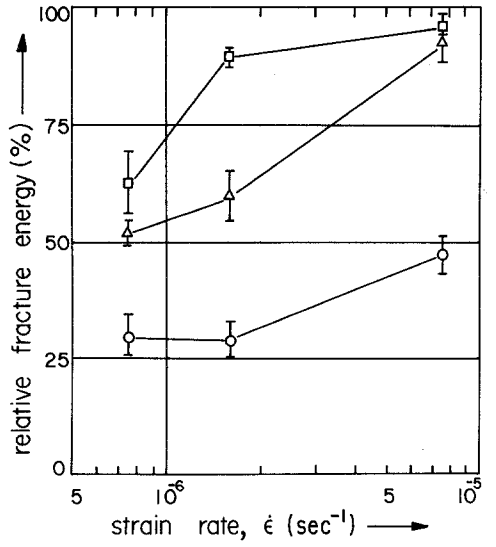

Figure 4 Strain-rate dependence of relative fracture energy in 3.5 wt % NaCl solution at 45° C, 33% cold-rolled specimens: ○ underaged in one stage 1.5 h at 160° C; △ peak-aged in two stages, 8 h at 108° C followed by 16 h at 160° C; □ overaged in two stages, 8 h at 108° C followed by 36 h at 160° C.

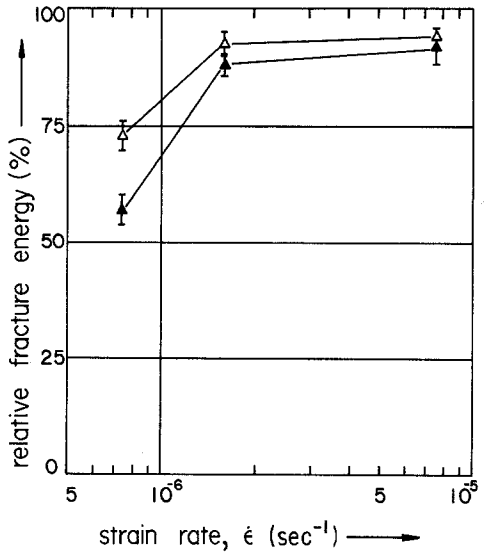

Figure 5 The strain-rate dependence of the relative fracture energy in 3.5 wt % NaCl solution at 30° C: △ 33% cold-rolled and then peakaged specimen; ▲ 75% cold-rolled and then peakaged specimen.

the interior of the specimen. As the strain rate decreased, i.e. $\dot{\epsilon} = 7.6 \times 10^{-7}$ sec^{-1}, the intercrystalline brittle fracture mode was to be a dominant feature. It is suggested that two stages of variation of relative fracture energy is a consequence of the change in the failure mode and results in the change of SCC resistance with decreasing strain rate.

The electrochemical attack goes through the anodic sites of gbs, at the same time, gbs act as stress concentrator due to the applied stress. As the strain rate decreases in the 1st stage, the repassivation rate at slip step tends to exceed the rate of slip step formation due to the stress at the gbs caused by straining, finally at the critical strain rate both rates will reach an equilibrium and this condition would be the most favourable for the SCC. Consequently the SCC resistance, as expressed by the relative fracture energy, would be a minimum at the critical strain rate as observed by Takano [26] in stainless steel and Buhl [27] in stainless steel, aluminium alloys and titanium alloys. Hence the influence of electrochemical dissolution of active sites, followed by the repassivation process, becomes more dominant in the first stage.

The estimation of mean SC crack propagation rate, assuming that SC intercrystalline fracture is fully brittle at the strain rate of $\dot{\epsilon} = 7.6 \times 10^{-7}$ sec^{-1} (4.2×10^{-5} mm sec^{-1}), gave $3 \sim 5 \times 10^{-6}$ mm sec^{-1} at 30° C and $4 \sim 6 \times 10^{-6}$ mm sec^{-1} at 45° C. This corresponds to a current density of 12 and 15 mA cm^{-2}, respectively, which does not exceed the strain rate of about 4.2×10^{-5} mm sec^{-1}. All these, in the preceding results, indicate that the electrochemical dissolution is the rate controlling process in the SCC.

The SCC resistance decreased as the testing temperature increased in the same trend as the strain rate dependence of the yield strength and work hardening, as seen in Figs. 3 and 4. As ageing proceeded from underaged, over peak-aged to overaged state, the SCC resistance increased at the constant strain rate, which accords with the results of SCC failure time measurements in alloy AA-7039 [28], i.e. technical Al–Zn–Mg alloy. The variation of SCC resistance with ageing state is related to the change of metallurgical parameters, such as ppt size in the gbs [1–4], distribution of solute atoms in the gbs [5–9], pfz width [10–13] and coherency of ppts in the grain [14–21].

The strain-rate dependence of relative fracture energy of 33 and 75% cold-rolled and then peak-aged specimens, is presented in Fig. 5. Both kinds of specimens were solutionized, then aged at the same temperature and for the same duration, but differed in their grain size on account of the different solutionizing time. It is assumed that all the solute atoms, magnesium and zinc, within the

same width of pfz, x, are precipitated at the gbs, since the same quench rate in both types of specimens are adopted, and $x \ll D$ (mean grain size). The estimation under this assumption yields nearly the same amount of solute atoms in the unit length of gbs of two degrees of cold-rolled specimens of different grain. The mean amount of solute atoms per unit length of gbs should be $c = 2x\rho(1 - x/D) \approx 2x\rho$, where x is the width of solute depleted zone, D, the mean grain diameter and ρ, the density of solute atoms at gbs. Moreover other metallurgical factors are nearly the same on account of the same solutionizing temperature and ageing treatments. The lower relative fracture energy is attributed to the small grain size in 75% cold-rolled specimens, i.e. larger electrochemical dissolution of anodic gbs area in the small grained specimen.

The apparent activation energy for SCC, H was calculated by using the following equation [29, 30]

$$(\sigma_1 - \sigma_2)_{\dot{\epsilon}} = \frac{H}{A}(\sigma_1 - \sigma_2)_T \qquad (1)$$

where $(\sigma_1 - \sigma_2)_{\dot{\epsilon}} = \Delta\sigma_{\dot{\epsilon}}$ is the stress increment due to the temperature change from $T_1 = 30°$ C to $T_2 = 45°$ C at the constant strain rate of $\dot{\epsilon}_1 = 7.6 \times 10^{-6}$ sec^{-1}, $(\sigma_1 - \sigma_2)_T = \Delta\sigma_T$ is the stress increment due to strain rate change from $\dot{\epsilon}_1 = 7.6 \times 10^{-6}$ sec^{-1} to $\dot{\epsilon}_2 = 7.6 \times 10^{-7}$ sec^{-1} at the constant temperature of $T_1 = 30°$ C, and H, the apparent activation energy for the mechanical process in oil and SCC processes in NaCl solution,

$$A = -RT^2 \frac{(\ln \dot{\epsilon}_1/\dot{\epsilon}_2)_T}{(T_1 - T_2)_{\dot{\epsilon}}} = 117\,115 \text{ J mol}^{-1}$$
$$T = 303 \text{ K} \qquad (2)$$

The activation energy, H, can be also determined from the slope of the best fit straight line in the plot of $\Delta\sigma_{\dot{\epsilon}}$ against $\Delta\sigma_T$ presented in Fig. 6, where the $\Delta\sigma_{\dot{\epsilon}}$ at a constant strain $\epsilon = 0.05$ to 0.1 was accociated with the $\Delta\sigma_T$ at the same strain ϵ. The plots yielded an activation energy of 47.5 kJ mol^{-1} for the peakaged and 51.5 kJ mol^{-1} for the overaged specimen in NaCl solution, and 103 kJ mol^{-1} for peakaged, 96.5 kJ mol^{-1} for overaged specimen in oil. The apparent activation energies for SCC estimated from the Arrhenius plot of inverse-SCC failure time in NaCl solution was shown to be much lower than those values for the peakaged and the overaged specimens determined by Equation 1.

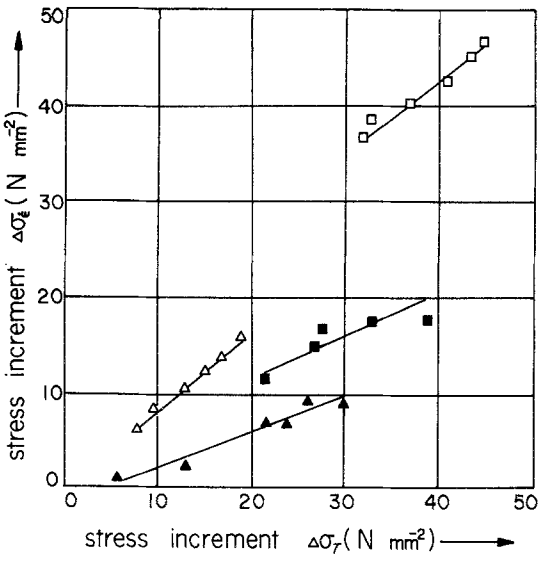

Figure 6 Stress increment, $\Delta\sigma_{\dot{\epsilon}}$, at constant strain rate against stress increment, $\Delta\sigma_T$, at constant test temperature: ▲ peakaged (in NaCl); ■ overaged (in NaCl); △ peakaged (in oil); □ overaged (in oil).

These differences may be attributed to the two different methods.

The activation energies of peakaged and overaged specimens in oil are similar to those for creep in pure aluminium and Al–3.2% Mg alloy (100.8 to 117.6 kJ mol^{-1}) [23, 31]. However, the activation energies for SCC in NaCl solution are similar to those for hydrogen diffusion in the aluminium alloy (46.2 to 54.6 kJ mol^{-1}) [31]/or anodic dissolution (43.3 to 60.5 kJ mol^{-1}) [31]. Therefore, it seems that the creep process is necessary for the occurrence of SCC in Al–Zn–Mg alloy. The difference, $H_{oil} - H_{SCC}$, is thought to be related to the thermally activated process for electrochemical attack in aqueous NaCl solution. Thus it is suggested that SCC processes are initiated by the rate controlled electrochemical dissolution of gbs and that cracks are propagated by mechanical processes such as creep.

4. Conclusion

The apparent activation energy for mechanical deformation in oil was 103 and 96.5 kJ mol^{-1} in the peakaged and overaged specimens, respectively, while those for SCC processes in NaCl solution were 47.5 and 51.5 kJ mol^{-1} in the peakaged and overaged specimens, respectively, indicating that the lower value of activation energy in the NaCl solution than in oil is caused by electrochemical dissolution. Average SC crack propagation rates

of AA-7039 in 3.5 wt % NaCl solution at the strain rate of about 4.2×10^{-5} mm sec^{-1} were estimated to be 3 to 5×10^{-6} mm sec^{-1} at 30° C and 4 to 6×10^{-6} mm sec^{-1} at 45° C, which is controlled by the electrochemical dissolution process. It is suggested that SCC in AA-7039 is composed of two steps, i.e. crack initiation by electrochemical dissolution and propagation by mechanical processes such as creep.

Acknowledgement

The authors are grateful to the Korea Science and Engineering Foundation, Seoul, for the financial support.

References

1. K. G. KENT, *J. Inst. Met.* 97 (1969) 127.
2. *Idem, J. Aust. Inst. Met.* **15** (1970) 171.
3. P. N. T. UNWIN and R. B. NICHOLSON, *Acta Metall.* 17 (1969) 1379.
4. P. N. ADLER, R. DEIASI and G. GESCHWIND, *Met. Trans.* **3** (1972) 3191.
5. I. T. TAYLOR and R. L. EDGAR, *ibid.* **2** (1971) 833.
6. P. DOIG and J. W. EDINGTON, *Met. Trans. A* **6A** (1975) 943.
7. *Idem, Corrosion-NACE* **31** (1975) 347.
8. P. DOIG, P. E. J. FLEWITT and J. W. EDINGTON, *ibid.* **33** (1977) 217.
9. W. GRUHL, B. GRZEMBA and L. RATKE, 7th International Leichtmetall-Tagung (Montanuniversität, Leoben, 1981) p. 124.
10. G. THOMAS and J. NUTTING, *J. Inst. Met.* 88 (1959–1960) 81.
11. A. J. SEDRIKS, P. W. SLATTERY and E. N. PUGH, *Trans. ASM* **62** (1969) 238.
12. *Idem, ibid.* **62** (1969) 815.
13. A. J. SEDRIKS, J. A. S. GREEN and D. L. NOVAK, *Met. Trans.* **1** (1970) 1815.
14. W. GRUHL, *Aluminium* **38** (1962) 775.
15. W. GRUHL and H. CORDIER, *Z. Metallkde.* **55** (1964) 577.
16. *Idem, Aluminium* **44** (1968) 403.
17. W. GRUHL and F. OSTERMANN, Berichte zum Symposium der Deutsche Gesellschaft Metallkunde, "Festigkeit metallischer Werkstoffe" (DGM, Bad Nauheim, 1974) pp. 387–410.
18. H. A. HOLL, *Corrosion-NACE* **23** (1967) 173.
19. M. O. SPEIDEL, *Phys. Status Solidus* **22** (1967) K71.
20. *Idem,* Proceedings of the Conference on Fundamental Aspects of SCC, The Ohio State University, September 1967 (NACE, Houston, Texas, 1969) pp. 561–79.
21. A. J. DE ARDO JR and R. D. TOWNSEND, *Met. Trans.* **1** (1970) 2573.
22. W. GRUHL, *Z. Metallkde.* **53** (1962) 670.
23. M. LANDKOF and L. GALOR, *Corrosion-NACE* **36** (1980) 241.
24. M. HENTHORNE and R. N. PARKINS, *Br. Corros. J.* **2** (1967) 186.
25. R. N. PARKINS, F. MAZZA, J. J. ROYUELA and J. SCULLY, *Werkst. Korros.* **23** (1972) 1020; 1124 [*Br. Corros. J.* 7 (1972) 154].
26. M. TAKANO, *Corrosion-NACE* **30** (1974) 441.
27. H. BUHL, *ASTM STP* **665** (1979) 333.
28. S. I. PYUN, *Metall.* 38(3) (1984) in press.
29. H. CONRAD and H. WIEDERSICH, *Acta. Metall.* 8 (1960) 128.
30. H. CONRAD, *J. Iron Steel Inst.* **198** (1961) 364.
31. W. W. GERBERICH and W. E. WOOD, *Met. Trans.* 5 (1974) 1295 (citation).

Received 29 July
and accepted 12 September 1983